Available online at www.sciencedirect.com
ScienceDirect
Polymer 49 (2008) 1220–1229
polymer
www.elsevier.com/locate/polymer

Aromatic diamine-based benzoxazines and their high performance thermosets

Ching Hsuan Lin*, Sheng Lung Chang, Chau Wei Hsieh, Hao Hsin Lee

Department of Chemical Engineering, National Chung Hsing University, 250, Kuo Kuang Road, Taichung 402, Taiwan

Received 11 August 2007; received in revised form 14 December 2007; accepted 25 December 2007
Available online 11 January 2008

Abstract

Four high-purity aromatic diamine-based benzoxazines (**13**–**16**), which could not easily be synthesized by traditional approaches, were successfully synthesized by a facile, widely useful three-step synthetic method using four typical aromatic diamines – 4,4′-diamino diphenyl methane (**1**), 4,4′-diamino diphenyl sulfone (**2**), 2,2-bis(4-(4-aminophenoxy)phenyl)propane (**3**), and bis(4-(4-aminophenoxy)phenyl)ether (**4**), respectively, as starting materials. The structures of the monomers (**5**–**16**) were confirmed by ^{1}H, ^{13}C, ^{1}H–^{1}H and ^{1}H–^{13}C NMR spectra. Their high performance thermosets, P(**13**–**16**), were obtained by thermal curing of benzoxazines (**13**–**16**), and their properties were studied and compared with polymer derived from bis(3,4-dihydro-2*H*-3-phenyl-1,3-benzoxazinyl)methane (**F-a**), a typical aromatic biphenol-based benzoxazine. Among the benzoxazines, **13** and **F-a** are constitutional isomers, but the T_g value and 5% decomposition temperature of P(**13**) are 53 and 111 °C, respectively, higher than those of P(**F-a**), demonstrating the power of the molecule-approach to enhance the thermal properties. Because of the large varieties of aromatic diamines, this approach can increase the molecule-design flexibility of benzoxazines.

Keywords: Benzoxazine; Thermoset; Curing

1. Introduction

Benzoxazine, a new thermosetting resin, can be polymerized by a thermally induced ring-opening reaction. Thermosets with low water absorption, superior electrical properties [1] and low surface energy [2] can be obtained after curing. According to the literature, most difunctional benzoxazines were synthesized from aromatic biphenols, monoamines and formaldehyde. The large varieties of aromatic biphenols and monoamines allow considerable molecule-design flexibility for benzoxazines. Some special functional groups can be introduced via biphenols or monoamines to provide some desired properties. For example, Takeichi and Agig prepared phenyl propargyl ether-based [3] and allylamine-based benzoxazines [4] to increase T_g and thermal stability. Ishida et al. synthesized acetylene [5,6], maleimide [7] and phenylphosphine oxide [8] containing benzoxazines to increase T_g, char yield and flame retardancy. Kimura et al. prepared a terpenediphenol-based benzoxazine to reduce water absorption and dielectric constant [9]. Chang and Su incorporated trifluoromethyl groups into benzoxazines to reduce the dielectric constant [10]. The common feature of these benzoxazines is that they are derived from aromatic biphenols, monoamines and formaldehyde. None of them are derived from aromatic diamines, phenol and formaldehyde. Benzoxazines based on difunctional [11–13], multifunctional aromatic amines or their derivatives [14] have seldom been discussed in the literature.

Ishida et al. reported the synthesis of bis(3,4-dihydro-2*H*-3-phenyl-1,3-benzoxazinyl) isopropane via 1,3,5-triarylhexahydro-1,3,5-triazine intermediate, which is generated by mixing stoichiometric amounts of paraformaldehyde and aniline at 70 °C for 35 min [15]. Therefore, if aromatic diamines and formaldehyde are reacted, an insoluble byproduct results due to the formation of a triazine network. In addition to the triazine network, condensations among methylol–methylol, methylol–amino or methylol–*ortho* hydrogen of aromatic

* Corresponding author. Tel.: +886 4 2285 0180; fax: +886 4 2285 4734.
E-mail address: linch@nchu.edu.tw (C.H. Lin).

0032-3861/$ - see front matter © 2008 Elsevier Ltd. All rights reserved.
doi:10.1016/j.polymer.2007.12.042

amine might also be responsible for the formation of the insoluble byproduct. A Japanese Patent revealed the manufacturing of benzoxazines from aromatic diamines and paraformaldehyde using solvents in which the aromatic diamine and paraformaldehyde have limited solubility [16]. The poor solubility of aromatic diamines and paraformaldehyde in the solvent reduced the formation of the triazine network and the condensations among methylol–methylol, methylol–amino or methylol–*ortho* hydrogen, while the formation of benzoxazine was not retarded due to the high concentration of phenol in the solvent. However, due to the solubility limitation, only benzoxazines based on 4,4′-diamino diphenyl methane and 4,4′-methylene-bis(2,6-dimethylaniline) were reported in the patent. No benzoxazines based on other aromatic diamines, such as 4,4′-diamino diphenyl sulfone, 2,2-bis(4-(4-aminophenoxy)phenyl)propane and bis(4-(4-aminophenoxy)-phenyl)ether, were prepared by this kinetic-controlled approach.

This work presents a clean and facile route for synthesizing high-purity aromatic diamine-based benzoxazines. Aromatic diamines with a weak electron-donating methylene group, a strong electron-withdrawing sulfone group and a strong electron-donating ether group were chosen as starting materials. Thus, four benzoxazines (**13**–**16**) derived from four typical aromatic diamines – 4,4′-diamino diphenyl methane (**1**), 4,4′-diamino diphenyl sulfone (**2**), 2,2-bis(4-(4-aminophenoxy)-phenyl)propane (**3**) and bis(4-(4-aminophenoxy)phenyl)ether (**4**), were prepared. The thermal properties of aromatic diamine-based polybenzoxazines were studied and compared with aromatic biphenol-based polybenzoxazines.

2. Experimental

2.1. Materials

Bis(3,4-dihydro-2*H*-3-phenyl-1,3-benzoxazinyl)methane (**F-a**) was kindly supplied by the Shikoku Corporation, Japan. 2-Hydroxybenzaldehyde (Showa), 4,4′-diamino diphenyl methane (**1**, Acros), 4,4′-diamino diphenyl sulfone (**2**, ChrisKev), 2,2-bis(4-(4-aminophenoxy)phenyl)propane (**3**, ChrisKev), bis-(4-(4-aminophenoxy)phenyl)ether (**4**, ChrisKev) and sodium borohydride ($NaBH_4$, Acros) were used as-received. *N*,*N*-Dimethylacetamide (DMAc) and *N*,*N*-dimethylformamide (DMF) were purchased from TEDIA, purified by distillation under reduced pressure over calcium hydride (Acros) and stored over molecular sieves. 1,4-Dioxane, chloroform and ethanol (99.5%) were purchased from various commercial sources and used without further purification.

2.2. Characterization

Differential scanning calorimetric (DSC) scans were obtained using a Perkin–Elmer DSC 7 in a nitrogen atmosphere at a heating rate of 20 °C/min. T_g was taken as the midpoint of the heat capacity transition between the upper and the lower points of deviation from the extrapolated liquids and glass lines. Thermogravimetric analysis (TGA) was performed using a Seiko Exatar 600 at a heating rate of 20 °C/min in a nitrogen atmosphere from 60 to 800 °C. NMR measurements were performed using a Varian Inova 600 NMR in DMSO-d_6. The assignment of individual peaks in ^1H and ^{13}C NMR spectra of compounds (**5**–**16**) was verified by the correlations in the gCOSY (^1H–^1H) and gHSQC (^1H–^{13}C) spectra.

2.2.1. Preparation and characterization of *5*

2-Hydroxybenzaldehyde (24.42 g, 0.2 mol), **1** (19.83 g, 0.1 mol) and DMAc (200 mL) were introduced into a 500 mL round bottom glass flask equipped with a nitrogen inlet and a magnetic stirrer. The reaction mixture was stirred at room temperature for 4 h. The precipitate was filtered and dried in a vacuum oven at 140 °C. Yellow powder (38.6 g, 95% yield) with a melting point of 219 °C (DSC) and a Δ enthalpy of 138 J/g was obtained. HR-MS (FAB^+) *m*/*z*, calcd. for $C_{27}H_{22}O_2N_2$: 406.1681; anal.: 407.1754, C27, 1H23, O2, N2. ^1H NMR (DMSO-d_6), $\delta = 4.04$ (2H, H^{12}), 6.94 (2H, H^2), 7.02 (2H, H^4), 7.25 (8H, H^9 and H^{10}), 7.38 (4H, H^1 and H^3), 8.63 (2H, H^7), 13.32 (2H, OH). ^{13}C NMR (DMSO-d_6), $\delta = 40.99$ (C^{12}), 117.21 (C^4), 119.03 (C^2), 119.20 (C^6), 121.33 (C^9), 129.87 (C^{10}), 132.18 (C^1), 133.05 (C^3), 139.79 (C^{11}), 146.62 (C^8), 161.08 (C^7), 162.16 (C^5). FTIR (KBr): 1618 cm^{-1} (C=N stretch), 3300–3500 cm^{-1} (OH stretch).

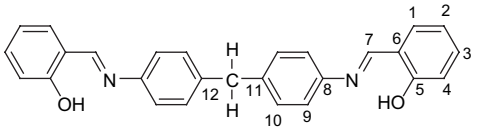

2.2.2. Preparation and characterization of *6*

Compound **6** was synthesized in a similar procedure of **5** using **2** as the starting material. Yellow powder (85% yield) with a melting point of 267 °C (DSC) and a Δ enthalpy of 129 J/g was obtained. HR-MS (FAB^+) *m*/*z*, calcd. for $C_{26}H_{20}O_4N_2S$: 456.1144; anal.: 457.1227, C26, 1H21, O4, N2, S. ^1H NMR (DMSO-d_6), $\delta = 6.98$ (2H, H^3), 7.01 (2H, H^2), 7.45 (2H, H^4), 7.58 (4H, H^9), 7.71 (2H, H^1), 8.04 (4H, H^{10}), 8.95 (2H, H^7), 12.40 (2H, OH). ^{13}C NMR (DMSO-d_6), $\delta =$ 116.73 (C^3), 119.92 (C^2), 122.59 (C^9), 128.87 (C^{10}), 132.41 (C^1), 134.10 (C^4), 138.62 (C^{11}), 153.14 (C^8), 160.24 (C^7), 165.60 (C^5). FTIR (KBr): 1617 cm^{-1} (C=N stretch), 3300–3500 cm^{-1} (OH stretch).

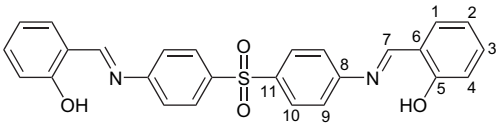

2.2.3. Preparation and characterization of *7*

Compound **7** was synthesized in a similar procedure of **5** using **3** as the starting material. Yellow powder (97% yield) was obtained. HR-MS (FAB^+) *m*/*z*, calcd. for $C_{41}H_{34}O_4N_2$: 618.2519; anal.: 619.2584, C41, 1H35, O4, N2. ^1H NMR (DMSO-d_6), $\delta = 1.63$ (6H, H^{17}), 6.95 (4H, H^{13}), 6.96 (4H, H^2 and H^4), 7.06 (4H, H^{10}), 7.24 (4H, H^{14}), 7.38 (2H, H^3), 7.43 (4H, H^9), 7.62 (2H, H^1), 7.93 (2H, H^7), 13.13 (2H,

OH). ^{13}C NMR (DMSO-d_6), $\delta = 30.55$ (C^{17}), 41.66 (C^{16}), 116.53 (C^4), 118.11 (C^{13}), 119.06 (C^2), 119.28 (2C, C^6 and C^{10}), 122.94 (C^9), 128.04 (C^{14}), 132.41 (C^1), 133.030 (C^3), 143.29 (C^{15}), 145.42 (C^8), 154.32 (C^{12}), 155.71 (C^{11}), 160.18 (C^7), 162.46 (C^5). FTIR (KBr): 1617 cm^{-1} (C═N stretch), 3250–3400 cm^{-1} (OH stretch).

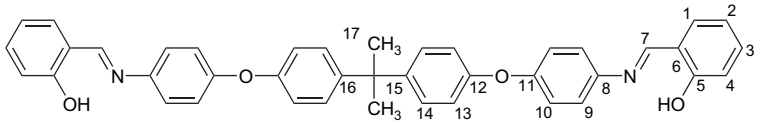

2.2.4. Preparation and characterization of **8**

Compound **8** was synthesized in a similar procedure of **5** using **4** as the starting material. Yellow powder (94% yield) with a melting point of 231 °C (DSC) and a Δ enthalpy of 144 J/g was obtained. HR-MS (FAB$^+$) *m/z*, calcd. for $C_{32}H_{24}O_4N_2$: 500.1736; anal.: 501.1822, C32, 1H25, O4, N2. Since **8** is insoluble in *d*-solvent of DMSO, $CDCl_3$, and acetone, no NMR data of **8** were available. FTIR (KBr): 1617 cm^{-1} (C═N stretch), 3300–3500 cm^{-1} (OH stretch).

2.2.5. Preparation and characterization of **9**

Compound **5** (32.52 g, 0.08 mol) and 250 mL of ethanol were introduced into a 500 mL round bottom glass flask equipped with a hydrogen balloon and a magnetic stirrer. $NaBH_4$ (3.23 g, 85.3 mmol) was added every 2 h. After $NaBH_4$ was added three times (85.3 mmol × 3), the reaction mixture was further stirred at room temperature for 10 h. The mixture was then poured into water (500 mL) with stirring, yielding a precipitate that was isolated by filtration. After the precipitate was dried, 31.1 g of off-white powder (95% yield) was obtained. HR-MS (FAB$^+$) *m/z*, calcd. for $C_{27}H_{26}O_2N_2$: 410.1994; anal.: 410.2004, C27, 1H26, O2, N2. ^{1}H NMR (DMSO-d_6), $\delta = 3.56$ (2H, H^{12}), 4.14 (4H, H^7), 5.74 (2H, NH), 6.47 (4H, H^9), 6.71 (2H, H^2), 6.79 (2H, H^4), 6.84 (4H, H^{10}), 7.02 (2H, H^3), 7.16 (2H, H^1), 9.48 (2H, OH). ^{13}C NMR (DMSO-d_6), $\delta = 39.78$ (C^{12}), 41.59 (C^7), 112.19 (C^9), 114.79 (C^4), 118.74 (C^2), 125.90 (C^6), 127.35 (C^3), 128.15 (C^1), 128.89 (C^{10}), 129.35 (C^{11}), 146.83 (C^8), 154.94 (C^5). FTIR (KBr): 1244 cm^{-1} (C–N stretch), 3290 cm^{-1} (NH stretch), 3400 cm^{-1} (OH stretch).

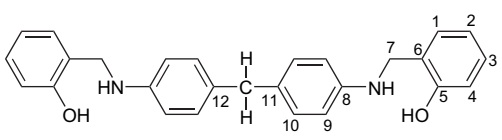

2.2.6. Preparation and characterization of **10**

Compound **10** was synthesized in a similar procedure of **9** using **6** as the starting material. Off-white (95% yield) powder with a melting point 134 °C (DSC) and a Δ enthalpy 51 J/g was obtained. HR-MS (FAB$^+$) *m/z*, calcd. for $C_{26}H_{24}O_4N_2S$: 460.1457; anal.: 461.1534, C 26, 1H25, O4, N2, S. ^{1}H NMR (DMSO-d_6), $\delta = 4.20$ (4H, H^7), 6.92 (NH), 6.60 (4H, H^9), 6.71 (2H, H^2), 6.81 (2H, H^4), 6.94 (2H, H^3), 7.09 (2H, H^1), 7.46 (4H, H^{10}), 9.56 (2H, OH). ^{13}C NMR (DMSO-d_6), $\delta = 40.77$ (C^7), 111.25 (C^9), 114.92 (C^4), 118.83 (C^2), 124.56 (C^{11}), 127.78 (C^1), 128.06 (C^6), 128.09 (C^3), 128.36 (C^{10}), 152.07 (C^8), 154.97 (C^5). FTIR (KBr): 1225 cm^{-1} (C–N stretch), 3410 cm^{-1} (NH stretch), 3500 cm^{-1} (OH stretch).

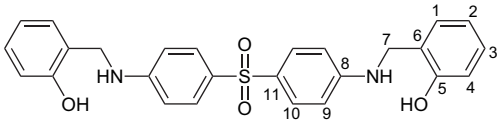

2.2.7. Preparation and characterization of **11**

Compound **11** was synthesized in a similar procedure of **9** using **7** as the starting material. Light yellow powder (96% yield) was obtained. HR-MS (FAB$^+$) *m/z*, calcd. for $C_{41}H_{38}O_4N_2$: 622.2832; anal.: 623.2904, C41, 1H39, O4, N2. ^{1}H NMR (DMSO-d_6), $\delta = 1.56$ (6H, H^{17}), 4.16 (4H, H^7), 5.90 (2H, NH), 6.58 (4H, H^9), 6.74 (6H, H^2 and H^{13}), 6.78 (4H, H^{10}), 6.81 (2H, H^4), 7.04 (2H, H^3), 7.11 (4H, H^{14}), 7.30 (2H, H^1), 9.51 (2H, OH). ^{13}C NMR (DMSO-d_6), $\delta = 30.69$ (C^{17}), 41.35 (C^{16}), 41.83 (C^7), 113.05 (C^9), 114.89 (C^4), 115.93 (C^{13}), 118.83 (C^2), 120.87 (C^{10}), 125.71 (C^{15}), 127.536 (C^3), 127.65 (C^{14}), 128.32 (C^1), 143.78 (C^6), 1475.71 (C^8), 145.74 (C^{11}), 155.03 (C^5), 156.65 (C^{12}). FTIR (KBr): 1244 cm^{-1} (C–N stretch), 3270 cm^{-1} (NH stretch), 3350 cm^{-1} (OH stretch).

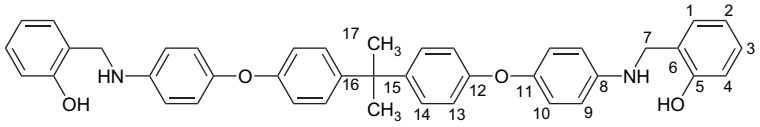

2.2.8. Preparation and characterization of **12**

Compound **12** was synthesized in a similar procedure of **9** using **8** as the starting material. White powder (96% yield) with a melting point of 183 °C (DSC) and a Δ enthalpy of 165 J/g was obtained. HR-MS (FAB$^+$) *m/z*, calcd. for $C_{32}H_{28}O_4N_2$: 504.2049; anal.: 505.2129, C32, 1H29, O4, N2. ^{1}H NMR (DMSO-d_6), $\delta = 4.16$ (4H, H^7), 5.88 (2H, NH), 6.58 (4H, H^9), 6.73 (2H, H^2), 6.77 (4H, H^{10}), 6.81 (4H, H^{13}), 6.82 (2H, H^4), 7.04 (2H, H^3), 7.20 (2H, H^1), 9.50 (2H, OH). ^{13}C NMR (DMSO-d_6), $\delta = 41.83$ (C^7), 113.03 (C^9), 114.86 (C^4), 118.13 (C^{13}), 118.77 (C^2), 120.21 (C^{10}), 125.70 (C^6), 127.48 (C^3), 128.28 (C^1), 145.48 (C^8), 146.57 (C^{11}), 153.36 (C^{12}), 155.02 (C^5). FTIR (KBr): 1215 cm^{-1}

(C–N stretch), 3265 cm^{-1} (NH stretch), 3390 cm^{-1} (OH stretch).

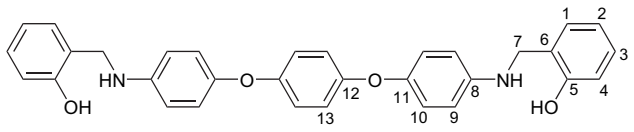

*2.2.9. Preparation and characterization of **13***

Compound **9** (20.53 g, 0.05 mol) and 150 mL of chloroform were introduced into a 250 mL round bottom glass flask equipped with a condenser and a magnetic stirrer. To this solution 8.11 g (0.1 mol) of 37% formaldehyde was added. The mixture was stirred at room temperature for 6 h and then further stirred at reflux temperature for 12 h. After that, the solution was dried over $MgSO_4$ and chloroform was removed using a rotary evaporator. Light yellow powder (>99% yield) with a melting point of 123 °C (DSC) and an exothermic peak temperature of 244 °C was obtained. HR-MS (FAB^+) *m/z*, calcd. for $C_{29}H_{26}O_2N_2$: 434.1994; anal.: 434.1987, C29, 1H26, O2, N2. ^1H NMR (DMSO-d_6), $\delta = 3.70$ (2H, H^{13}), 4.58 (4H, H^7), 5.37 (4H, H^8), 6.69 (4H, H^{10}), 6.84 (2H, H^2), 7.01 (2H, H^3), 7.02 (2H, H^4), 7.04 (2H, H^1), 7.07 (4H, H^{11}). ^{13}C NMR (DMSO-d_6), $\delta = 39.92$ (C^{13}), 49.01 (C^7), 78.87 (C^8), 116.14 (C^{10}), 117.57 (C^3), 120.33 (C^2), 121.25 (C^6), 127.10 (C^{11}), 127.56 (C^1), 129.15 (C^4), 133.80 (C^{12}), 145.84 (C^9), 153.89 (C^5). FTIR (KBr): 939 cm^{-1} (N–C–O stretch), 1032 cm^{-1} (Ar–O–C symmetric stretch), 1225 cm^{-1} (Ar–O–C asymmetric stretch), 1370 cm^{-1} (C–N stretch).

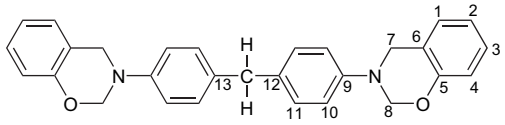

*2.2.10. Preparation of **13** by a solvent-less approach*

Compound **9** (12.31 g, 0.03 mol) and 1.98 g (0.066 mol) of paraformaldehyde were introduced into a 250 mL round bottom glass flask. The mixture was rotated and mixed at 140 °C for 1 h by a rotary evaporator and then further reacted at reduced pressure (5 mmHg) for 2 h to remove excess paraformaldehyde and the resulting water. The yield was quantitative. Benzoxazine (**13**) prepared by this approach has the same NMR spectra as that prepared in chloroform.

*2.2.11. Preparation and characterization of **14***

Compound **14** was synthesized in chloroform by a similar procedure of **13** using **10** as the starting material. Light yellow powder (>99% yield) with a melting point of 209 °C (DSC) and an exothermic peak temperature of 261 °C was obtained. HR-MS (FAB^+) *m/z*, calcd. for $C_{28}H_{24}O_4N_2S$: 484.1457; anal.: 485.1545, C28, 1H25, O4, N2, S. ^1H NMR (DMSO-d_6), $\delta = 4.71$ (4H, H^7), 5.47 (4H, H^8), 6.74 (2H, H^4), 6.88 (2H, H^2), 7.08 (2H, H^3), 7.11 (2H, H^1), 7.23 (4H, H^{10}), 7.71 (4H, H^{11}). ^{13}C NMR (DMSO-d_6), $\delta = 48.09$ (C^7), 76.95 (C^8), 115.96 (C^{10}), 116.37 (C^4), 120.78 (C^2), 120.96 (C^6), 127.20 (C^1), 127.77 (C^3), 128.56 (C^{11}), 131.99 (C^{12}), 151.07 (C^9), 153.62 (C^5). FTIR (KBr): 954 cm^{-1} (N–C–O stretch), 1035 cm^{-1} (Ar–O–C symmetric stretch), 1228 cm^{-1} (Ar–O–C asymmetric stretch), 1375 cm^{-1} (C–N stretch).

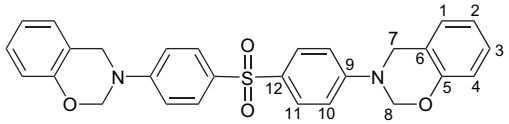

*2.2.12. Preparation and characterization of **15***

Compound **15** was synthesized in chloroform by a similar procedure of **13** using **11** as the starting material. Light yellow powder (>99% yield) was obtained. HR-MS (FAB^+) *m/z*, calcd. for $C_{43}H_{38}O_4N_2$: 646.2832; anal.: 647.2917, C43, 1H39, O4, N2. ^1H NMR (DMSO-d_6), $\delta = 1.57$ (6H, H^{18}), 4.61 (4H, H^7), 5.39 (4H, H^8), 6.73 (2H, H^4), 6.79 (4H, H^{10}), 6.86 (2H, H^2), 6.90 (4H, H^{14}), 7.08 (2H, H^3), 7.09 (2H, H^1), 7.12 (4H, H^{11}), 7.13 (4H, H^{15}). ^{13}C NMR (DMSO-d_6), $\delta = 30.58$ (C^{18}), 41.44 (C^{17}), 49.30 (C^7), 79.10 (C^8), 116.20 (C^4), 116.98 (C^{10}), 119.11 (C^{11}), 119.96 (C^{14}), 120.42 (C^2), 121.15 (C^6), 127.13 (C^1), 127.62 (C^3), 127.78 (C^{15}), 144.04 (C^9), 144.52 (C^{16}), 150.02 (C^{12}), 153.90 (C^{13}), 155.39 (C^5). FTIR (KBr): 939 cm^{-1} (N–C–O stretch), 1035 cm^{-1} (Ar–O–C symmetric stretch), 1226 cm^{-1} (Ar–O–C asymmetric stretch), 1380 cm^{-1} (C–N stretch).

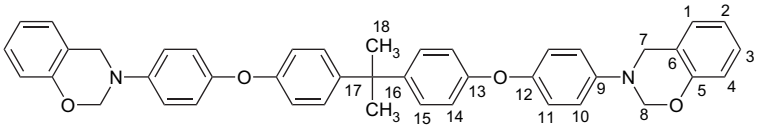

*2.2.13. Preparation and characterization of **16***

Compound **16** was synthesized in chloroform by a similar procedure of **13** using **12** as the starting material. Yellow powder (>99% yield) with a melting point of 164 °C (DSC) and an exothermic peak temperature of 240 °C was obtained. HR-MS (FAB^+) *m/z*, calcd. for $C_{34}H_{28}O_4N_2$: 528.2049; anal.: 529.2129, C34, 1H29, O4, N2. ^1H NMR (DMSO-d_6), $\delta = 4.61$ (4H, H^7), 5.39 (4H, H^8), 6.72 (2H, H^5), 6.86 (2H, H^3), 6.89 (4H, H^{10}), 6.91 (4H, H^{14}), 7.08 (2H, H^4), 7.09 (2H, H^2), 7.12 (4H, H^{11}). ^{13}C NMR (DMSO-d_6), $\delta = 49.32$ (C^7), 79.13 (C^8), 116.18 (C^5), 119.17 (C^{11}), 119.36 (C^{14}), 119.38 (C^{10}), 120.42 (C^3), 121.17 (C^1), 127.14 (C^2), 127.63 (C^4), 143.87 (C^9), 150.71 (C^{12}), 152.67 (C^{13}), 153.89 (C^6). FTIR (KBr): 946 cm^{-1} (N–C–O stretch), 1054 cm^{-1} (Ar–O–C symmetric stretch), 1227 cm^{-1} (Ar–O–C asymmetric stretch), 1371 cm^{-1} (C–N stretch).

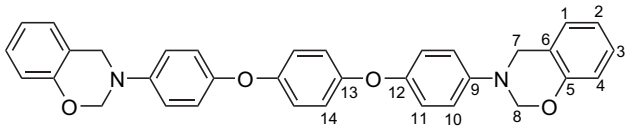

2.3. Preparation of polybenzoxazines

Benzoxazines (**13**–**16**) or **F-a** was melted, stirred and transferred to an aluminum mold and then cured at 160, 180, 200 and 220 °C for 2 h each in an air-circulating oven. Thereafter, samples were allowed to cool slowly to room temperature to prevent cracking.

3. Results and discussion

3.1. Synthesis and characterization of monomers

To prevent the formation of gelation, the direct contact between aromatic diamines and formaldehyde should be avoided. Thus, in the first step, 2-hydroxybenzaldehyde was chosen to react with aromatic diamines (**1**–**4**), yielding **5**–**8** with an *o*-hydroxy phenylimine linkage (Scheme 1). The reaction occurred at room temperature without any catalyst and the yield depends on the nucleophilic ability of aromatic diamines. Amines with a weak electron-donating methylene group (**1**) or a strong electron-donating ether group (**3**–**4**) result in high yield (94–97%). The ^{1}H and ^{13}C NMR spectra of **6** and the assignment of each peak are shown in Fig. 1. As shown in Fig. 1, a signal at 8.95 ppm standing for imine linkage appeared as the aldehyde signal of 2-hydroxybenzaldehyde at 10.80 ppm disappeared, indicating the formation of an imine linkage. A phenolic OH signal at 12.40 ppm appeared as the phenolic OH signal of 2-hydroxybenzaldehyde at 10.2 ppm disappeared. The phenolic OH–imine resonance, which lowers the electron density of phenolic OH, is responsible for the downshift of chemical shift, further confirming the formation of an imine linkage.

In the second step, the imine linkage of **5**–**8** was reduced, yielding **9**–**12** with a secondary amine structure. At first, hydrogen was used to reduce the imine linkage, but no reaction occurred. Then, sodium borohydride was employed to reduce the imine linkage, and the reaction took place at room temperature with a high yield (95–96%). The equivalent ratio of sodium borohydride to imine linkage was 1.6 to ensure that the reduction can be complete. Since sodium borohydride is water soluble, the reaction mixture was poured into water to remove residual sodium borohydride after the reaction was complete. The ^{1}H and ^{13}C NMR spectra of **10** and the assignment of each peak are shown in Fig. 2. As shown in Fig. 2, a signal at 9.56 ppm appeared as the phenolic OH signal of **6** at 12.40 ppm disappeared. The upshift of chemical shift is reasonable because the phenolic OH–imine resonance was destroyed after the reduction. Besides, two new peaks at 6.92 and 4.20 ppm standing for the CH_2–N*H* and CH_2–NH, respectively, appeared as the imine signal of **6** at 8.95 ppm disappeared, further confirming the reduction of imine linkage.

In the third step, formaldehyde was added [17] to the chloroform solution of **9**–**12** to react with the secondary amine at room temperature, resulting in a presumable intermediate with a hydroxymethylamine (NCH_2OH) structure. Thereafter, the reaction temperature was raised to induce the ring closure condensation between the hydroxymethylamine and the *o*-hydroxy groups, forming benzoxazines (**13**–**16**). This reaction can be conducted with quantitative yield in dioxane, toluene or even chloroform at the reflux temperature of each solvent. However, dioxane is very difficult to remove from **14**, even after drying at 150 °C for 8 h, according to the DSC thermogram and the NMR spectrum. Chloroform is the best solvent for this

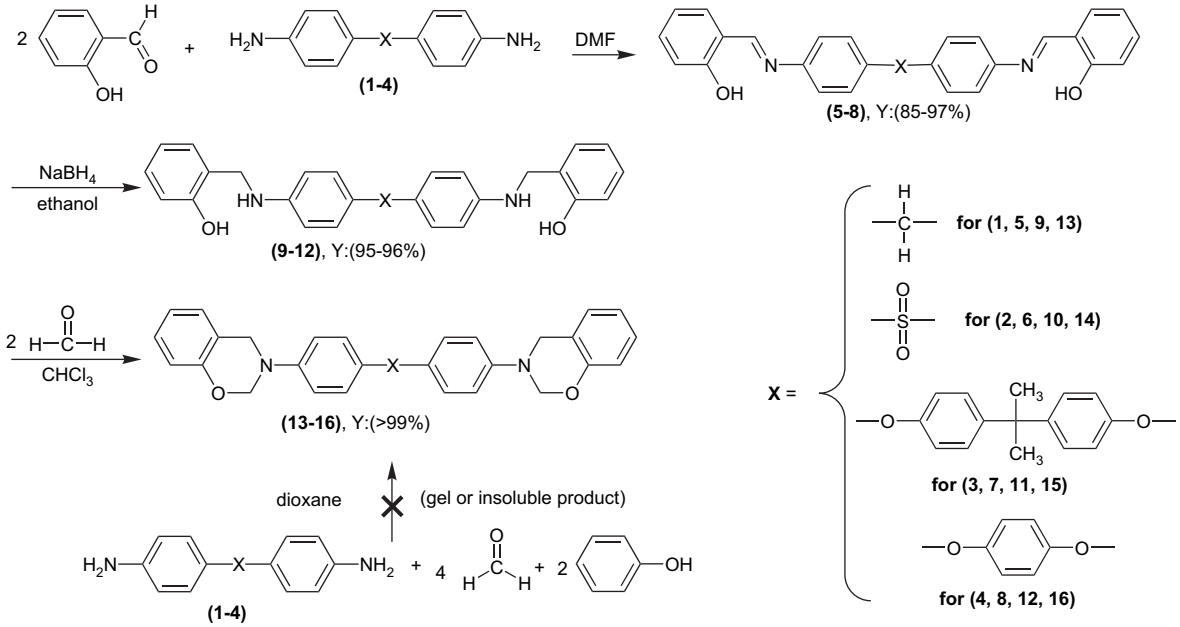

Scheme 1. Synthesis of benzoxazines (**13**–**16**).

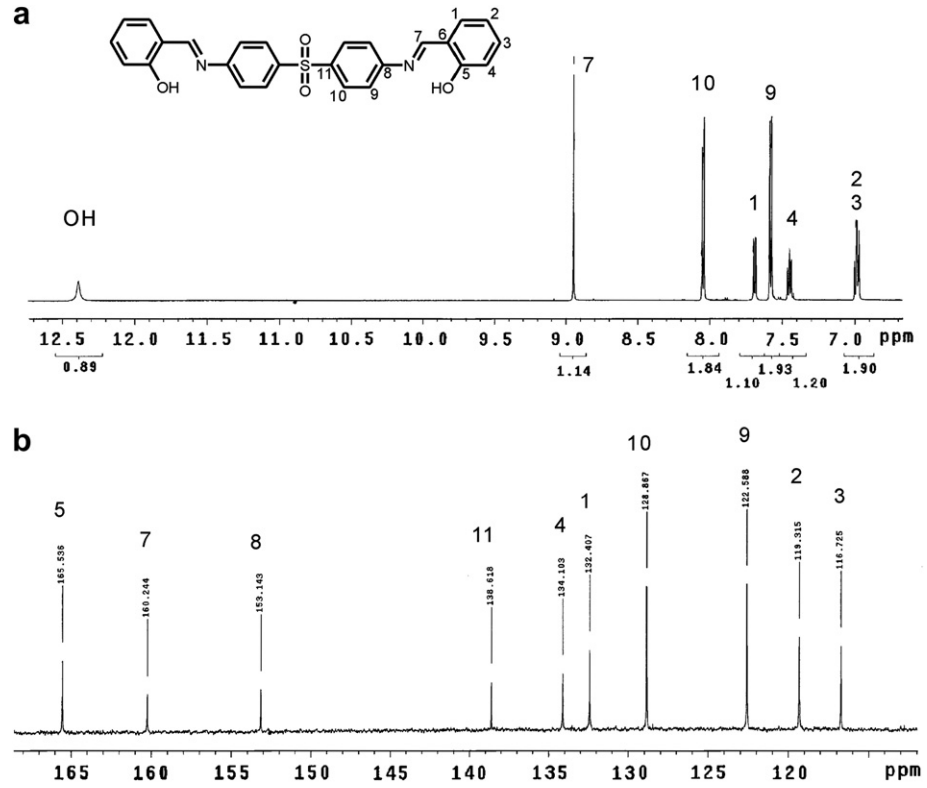

Fig. 1. (a) ^{1}H and (b) ^{13}C NMR spectra of **6**.

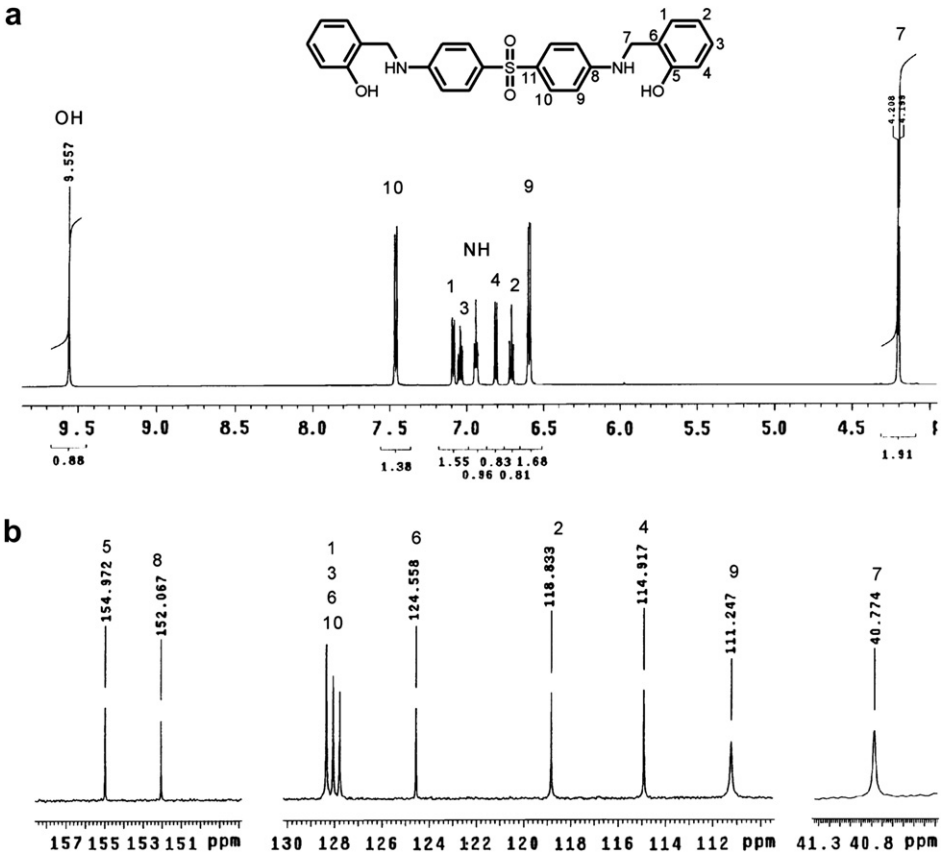

Fig. 2. (a) ^{1}H and (b) ^{13}C NMR spectra of **10**.

reaction because the immiscibility of chloroform with water promotes the completion of this reaction [18]. Additionally, the low boiling point of chloroform makes it easy to be removed by a rotary evaporator. The ^{1}H and ^{13}C NMR spectra of **14** and the assignment of each peak are shown in Fig. 3. As shown in Fig. 3, the appearance of characteristic peaks at 5.39 and 4.61 ppm standing for the O–CH_2–N and Ph–CH_2–N of oxazine, respectively, verifies the formation of benzoxazines. No signal corresponding to N–CH_2–Ph at around 3.80 ppm resulting from the ring opening of benzoxazine was observed [19], revealing the purity of synthesized benzoxazines. Generally, conventional aromatic biphenol-based benzoxazines often need two extraction procedures to remove insoluble oligomer and unreacted monomers. However, no extraction or purification is required to yield high-purity benzoxazines by this approach. As discussed in Section 1, besides the triazine network, the condensations among methylol–methylol, methylol–amino and methylol–*ortho* hydrogen of aromatic amine might also be responsible for the formation of the insoluble byproduct. However, a methylol structure was also resulted in this approach. This reminds us that the gelation occurring in the direct reaction of aromatic diamine, phenol and formaldehyde is not resulted from the methylol–methylol and methylol–amino condensations. Furthermore, benzoxazines based on aliphatic diamine can easily be synthesized without gelation [20], suggesting no methylol–methylol and methylol–amine condensations. Thus, the condensation between the methylol–*ortho* hydrogen of aromatic amine, along with the triazine network might be the major reasons of gelation for aromatic diamine-based benzoxazines when they are synthesized by a traditional approach.

3.2. DSC thermograms of benzoxazines

Fig. 4 shows the DSC thermograms of benzoxazines (**13**–**16**) and **F-a**. As aromatic biphenol-based benzoxazine (**F-a**) do, the aromatic diamine-based benzoxazines (**13**–**16**) show apparent exotherms in the range 239–261 °C, demonstrating the thermal curing characteristic. The melting point of **13** is 123 °C, while the exothermic peak temperature is 244 °C. The wide processing window makes **13** easy to process. Due to the low melting point and high exothermic curing temperature, benzoxazine (**13**) can be synthesized by a melting (solvent-less) method [14] at 140 °C, making it industrially interesting. Benzoxazines (**15**–**16**), with flexible ether group, also show wide processing temperature. In contrast, benzoxazine (**14**), which has a melting point and exothermic peak temperature of 209 and 261 °C, respectively, shows a smaller processing window than other benzoxazines do. The polar sulfonyl group, which reduces the entropy change (ΔS) for the melting process, increases the melting point.

3.3. Curing of benzoxazines probed by IR

Fig. 5 shows IR spectra of **13** after cumulative curing at each temperature for 20 min. After curing at 220 °C, the

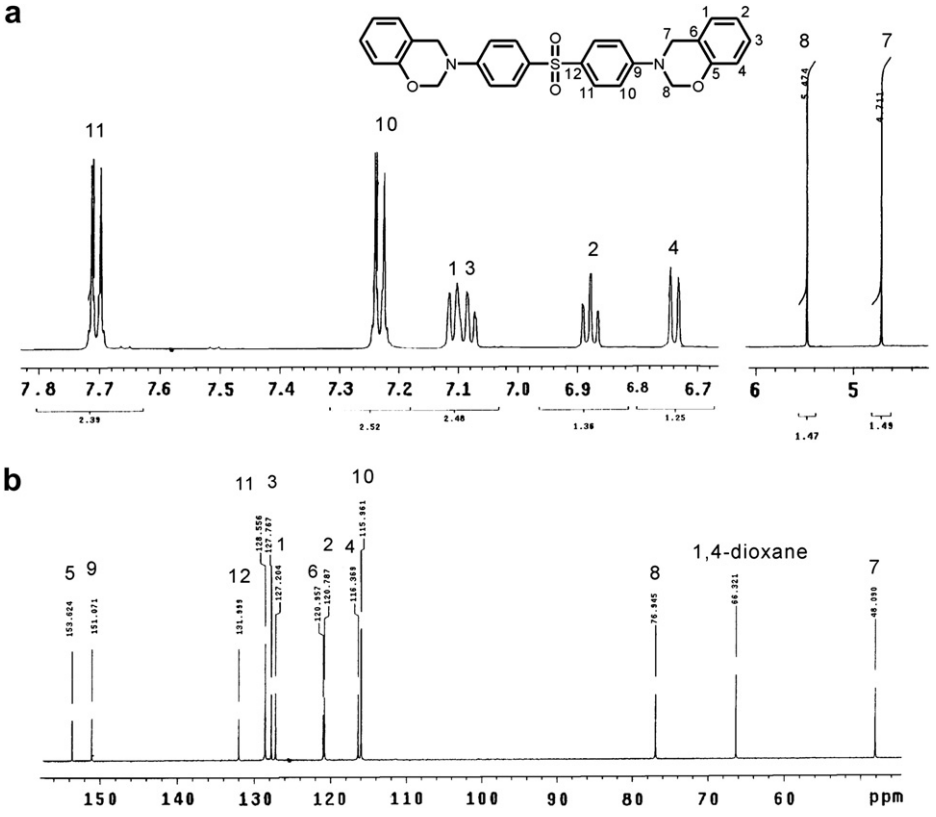

Fig. 3. (a) ^{1}H and (b) ^{13}C NMR spectra of **14**.

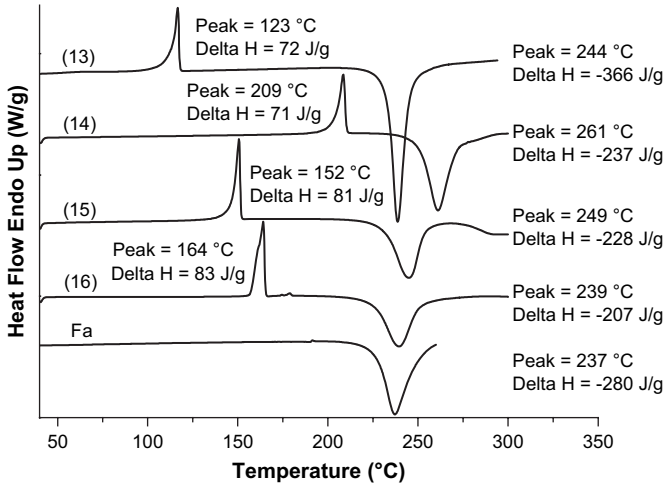

Fig. 4. DSC thermograms of benzoxazines **13**–**16** and **F**-**a**.

Ar–O–C absorptions at 1032 and 1225 cm^{-1}, the oxazine absorptions at 939 and 1370 cm^{-1}, and the *ortho*-substituted benzene absorptions at 1610 and 1513 cm^{-1} disappeared, but the 1,2,3-trisubstituted benzene absorptions at 1616 and 1504 cm^{-1} appeared. In comparison with **F**-**a** curing system, in which the Ar–O–C absorptions at 1030 and 1225 cm^{-1}, the oxazine absorptions at 945 and 1367 cm^{-1} and the 1,2,4-trisubstituted benzene absorption at 1499 cm^{-1} disappeared after 220 °C curing, we conclude that the structure of P(**F**-**a**) and P(**13**) is quite different, even though **F**-**a** and **13** are constitutional isomers. According to the IR analysis, the structure of P(**13**) was proposed and is shown in Scheme 2. The nitrogen linkage in P(**F**-**a**) is linked to a phenyl pendant, but the nitrogen linkage in P(**13**) is bonded to the other repeating unit. The difference in structure has a huge influence on thermal properties and will be discussed later.

3.4. Thermal properties of polybenzoxazines

T_gs of P(**13**–**16**) and P(**F**-**a**) were measured by DSC, and the result is listed in Table 1. T_g of P(**13**) is 208 °C, which is 53 °C higher than that of P(**F**-**a**). As shown in Scheme 2, the nitrogen linkage of P(**13**), instead of bonding to a phenyl pendant, is bonded to the other repeating unit, leading to a small segmental mobility, and explaining the higher T_g of P(**13**). Instead of enhancing T_g value of polybenzoxazines by incorporating curable propargyl ether [3], allyl [4], and maleimide functional groups [7,21,22], which may decrease the toughness of polybenzoxazines due to the higher crosslinking density, this work demonstrates the power of the molecule-approach to enhance T_g. The T_gs of P(**15**) and P(**16**) are 170 and 172 °C, which are lower than that of P(**13**) because of the presence of a flexible ether group and higher molecular weight between two crosslink points. T_g of P(**14**) is 184 °C after curing at 220 °C, which is not as high as expected although a polar sulfonyl group exists in its structure. One possible explanation for the unexpected low T_g is related to the high melting point (209 °C) of the benzoxazine (**14**). During the curing cycle at 160 (2 h), 180 (2 h) and 200 °C (2 h), no obvious curing reaction took place because the benzoxazine is crystalline. The curing reaction occurred only in the last curing cycle (2 h at 220 °C), making incomplete curing conversion. As a result, we raise the curing temperature to increase the conversion. The T_g of P(**14**) increases from 184 to 190 °C after curing at 240 °C (2 h), and to 201 °C after curing at 260 °C (2 h).

Fig. 6 shows the TGA thermograms of P(**13**–**16**) and P(**F**-**a**), and the result is listed in Table 1. The 5% degradation temperature of P(**13**) is 425 °C, which is 111 °C higher than that of P(**F**-**a**). The char yield at 800 °C is 52%, which is extremely high for polymers. According to the literature, the 5% degradation temperature of conventional polybenzoxazines rarely

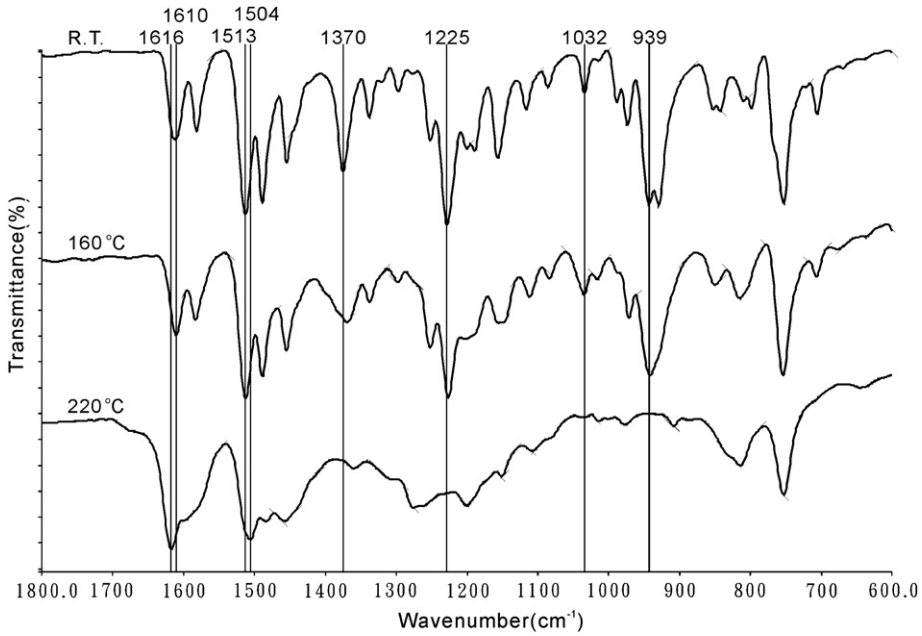

Fig. 5. IR spectra of **13** after cumulative curing at each temperature for 20 min.

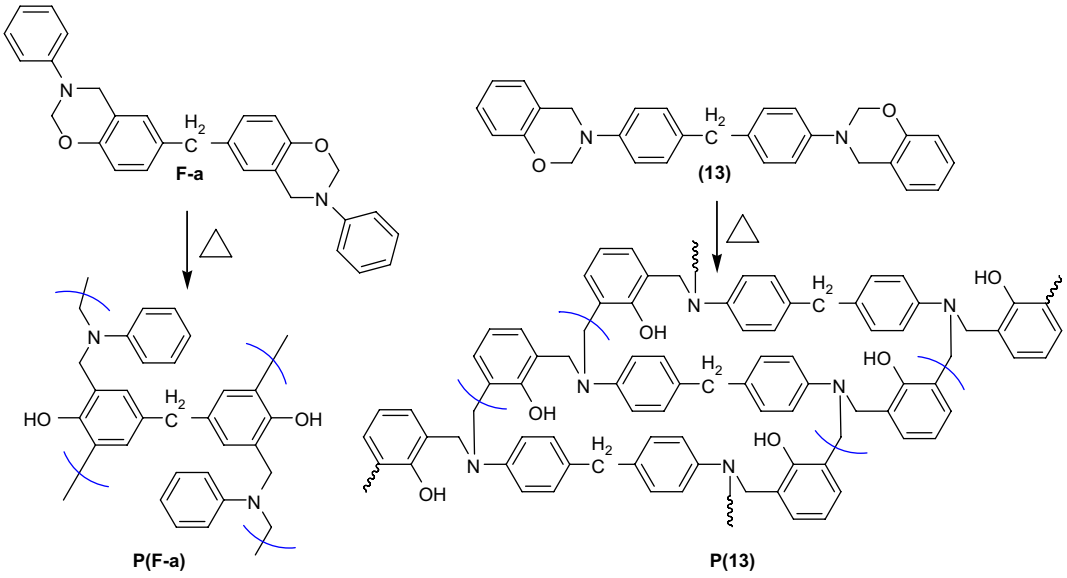

Scheme 2. Ideal structure of P(**F-a**) and P(**13**).

exceeds 350 °C, and the release of aniline fragment is responsible for the low thermal stability of polybenzoxazines [23–25]. Therefore, the introduction of a cross-linkable site into aniline, such as ethylnyl [26,27], propargyl ether [3], and nitrile group [6], has been proved an effective way to enhance the thermal stability of polybenzoxazines. As shown in Scheme 2, the nitrogen linkage in P(**13**) is bonded to the other repeating unit, making the release of aniline fragment difficult, and causing P(**13**) thermally more stable than P(**F-a**). The 5% degradation temperature and char yield of P(**14–16**) are also very high, further demonstrating the high thermal stability of aromatic diamine-based polybenzoxazines.

Table 1
Thermal properties of P(**13–16**) and P(**F-a**) thermosets

Benzoxazine	T_m [a] (°C)	T_{peak} [b] (°C)	T_g [c] (°C)	T_d [e] (°C)	Char yield[f] (%)
13	123	244	208	425	52
14	209	261	184 (201)[d]	382	62
15	152	249	170	412	46
16	164	239	172	417	62
F-a	–	237	155	314	49

[a] Melting point of benzoxazine.
[b] Exothermic peak temperature of benzoxazine.
[c] T_g value of corresponding polybenzoxazines after curing at 220 °C (2 h).
[d] T_g value after curing at 260 °C (2 h).
[e] The 5% decomposition temperature of corresponding polybenzoxazines in a nitrogen atmosphere.
[f] Residual weight percentage of corresponding polybenzoxazine at 800 °C in a nitrogen atmosphere.

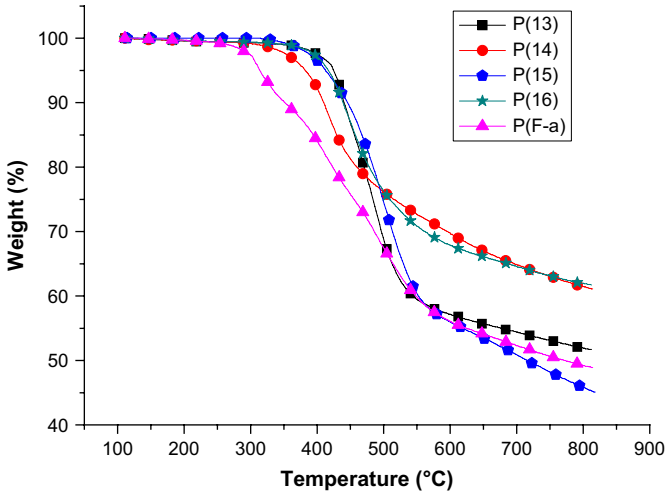

Fig. 6. TGA thermograms of P(**13–16**) and P(**F-a**).

4. Conclusion

Aromatic diamine-based benzoxazines, which could not easily be synthesized by traditional approaches, were successfully prepared by a widely useful three-step procedure using inexpensive raw materials. The new benzoxazines can be polymerized similarly to conventional aromatic biphenol-based benzoxazines and tend to yield structures with higher T_g and better thermal stability. Although, at this moment, a three-step procedure is required to maintain high purity of benzoxazines, this approach can theoretically be simplified into a one-pot procedure in the future. The large variety of aromatic diamines enables this approach to increase the molecule-design flexibility of benzoxazines.

Acknowledgments

The authors would like to thank the National Science Council of the Republic of China, Taiwan for financial support. Partial sponsorship by the Green Chemistry Project (NCHU), funded by the Ministry of Education, is also gratefully acknowledged.

References

[1] Ishida H, Allen DJ. J Polym Sci Part B Polym Phys 1996;34:1019.
[2] Wang CF, Su YC, Kuo SW, Huang CF, Sheen YC, Chang FC. Angew Chem Int Ed 2006;45:2248.

[3] Agig T, Takeichi T. Macromolecules 2001;34:7257.
[4] Agig T, Takeichi T. Macromolecules 2003;36:6010.
[5] Brunovska Z, Lyon R, Ishida H. Thermochim Acta 2000;357:195.
[6] Brunovska Z, Ishida H. J Appl Polym Sci 1999;73:2937.
[7] Ishida H, Ohba S. Polymer 2005;46:5588.
[8] Choi SW, Ohba S, Brunovska Z, Hemvichian K, Ishida H. Polym Degrad Stab 2006;91:1166.
[9] Kimura H, Murata Y, Matsumoto A, Hasegawa K, Ohtsuka K, Fukuda A. J Appl Polym Sci 1999;74:2266.
[10] Su YC, Chang FC. Polymer 2003;44:7989.
[11] Shen SB, Ishida H. J Appl Polym Sci 1996;61:1595.
[12] Takeichi T, Kano T, Agag T. Polymer 2005;46:12172.
[13] Men W, Lu Z. J Appl Polym Sci 2007;106:2769.
[14] Subrayan RP, Jones FN. Chem Mater 1998;10:3506.
[15] Brunovska Z, Liu JP, Ishida H. Macromol Chem Phys 1999;200:1745.
[16] Koichi N, Masaaki O, Kenji O. (Matsushita Electric Works) JP Kokai 2005-213301;2005.
[17] Burke WJ. J Am Chem Soc 1949;71:609.
[18] Ishida H, Low HY. J Appl Polym Sci 1998;69:2559.
[19] Ishida H, Ning X. J Polym Sci Part A Polym Chem 1994;32:1121.
[20] Allen DJ, Ishida H. J Appl Polym Sci 2006;101:2798.
[21] Agag T, Takeichi T. J Polym Sci Part A Polym Chem 2006;44:1424.
[22] Liu YL, Yu JM, Chou CI. J Polym Sci Part A Polym Chem 2004;42:5954.
[23] Kimura H, Matsumoto A, Hasegawa K, Ohtsuka K, Fukuda A. J Appl Polym Sci 1997;68:1903.
[24] Ishida H, Hemvichian K. Polymer 2002;43:4391.
[25] Low HY, Ishida H. Polymer 1999;40:4365.
[26] Kim HJ, Brunovska Z, Ishida H. Polymer 1999;40:1815.
[27] Kim HJ, Brunovska Z, Ishida H. Polymer 1999;40:6565.